Energy 284 (2023) 128559

Contents lists available at ScienceDirect

Energy

journal homepage: www.elsevier.com/locate/energy

Oxy-combustion characteristics of torrefied biomass and blends under O_2/N_2, O_2/CO_2 and $O_2/CO_2/H_2O$ atmospheres

Luis I. Díez *, Alexander García-Mariaca, Paula Canalís, Eva Llera

Department of Mechanical Engineering, University of Zaragoza, María de Luna s/n, 50018, Zaragoza, Spain

ARTICLE INFO

Keywords:
Oxy-combustion
Torrefied biomass
Entrained-flow reactor
Burnout
NO_x emissions

ABSTRACT

The combined use of bio-fuels along with CO_2 capture techniques is the basis for the so-called negative emissions energy systems. In this paper, oxy-fuel combustion of two torrefied biomasses is experimentally investigated in a lab-scale entrained flow reactor. The torrefied biomasses are fired alone, and co-fired with coal (50%). Two oxygen concentrations (21% and 35%) and four steam concentrations are tested: 0% (dry recycle oxy-combustion), 10% (wet recycle oxy-combustion), 25% and 40% (towards the concept of oxy-steam combustion). The tests are designed to get the same mean residence time for all the fuels and conditions. Burnout degrees are significantly increased (up to 9 and 16 percentage points) when the share of torrefied biomass is raised, with a slightly better behavior of the torrefied pine in comparison to the torrefied agro-biomass. C-fuel conversion to CO_2 follows a similar trend to the observed for the burnout degrees. NO formation rates are reduced when oxy-firing torrefied biomass alone in comparison to the blends, with maximum diminutions of 16.9% (torrefied pine) and 8.5% (torrefied agro-biomass). As regards the effect of steam, the best results are found for the 25% H_2O atmospheres in most of the cases, yielding maximum conversions along with minimum NO levels.

1. Introduction

Decarbonization of energy systems is a key challenge to cope with the urgent reduction of CO_2 emissions required to mitigate the impact of global warming. In this context, biomass resources can contribute to progressively deplete the use of fossil fuels and, in particular, the use of coal for power generation in large scale utility plants. The replacement of coal by biomass in existing installations brings along outstanding environmental benefits, but also constrains related to lower calorific values of the fuels [1–3] or operative problems, such as slagging, fouling or corrosion that some mineral matter present in the biomass may promote [4,5]. Some of these issues can be attenuated by using torrefied biomass, which also offers other advantages like better homogeneity, grindability and hydrophobicity [6].

On the other hand, CO_2 capture techniques represent another suitable decarbonization option. The combination of a CO_2-neutral biofuel along with a capture and storage system (Bio-CCS) would lead to negative emissions technologies [7]. One of the alternatives with a wider margin of optimization is the oxy-fuel combustion [8,9]. More recently, CO_2 replacement by H_2O has been highlighted as an improved oxy-fuel combustion approach, the so-called oxy-steam combustion. It consists on the recirculation of condensed water to the boiler, which is re-evaporated to serve as oxygen diluting and temperature moderator, and then avoiding the flue gas recycling [10,11]. So far, oxy-fuel combustion of pulverized coal has been extensively studied from a lot of lab-scale facilities to some demo-scale plants [8,12,13]. The effects caused by H_2O enrichment are also receiving some attention in recent years by fundamental studies for coal oxy-steam combustion [14–20], but the experiences including biomass are still very scarce.

Regarding fuel conversion, Gil et al. [21] studied the effects of H_2O addition on coal and biomass oxy-combustion by thermogravimetry. They obtained that substituting up to a 40% of CO_2 by H_2O increases the mass-loss rate, augments the reactivity and decreases the combustion time. Lei et al. [22] developed combustion experiments of single particles of sewage sludge/pine sawdust and sewage sludge/bituminous coal in O_2/N_2, O_2/CO_2 and $O_2/CO_2/H_2O$ atmospheres. These authors proved that H_2O presence (up to 30%) increases combustion temperature and decreases burnout time of the blends. Rabaçal et al. [23] investigated isolated particles fragmentation of black acacia charcoal and two sub-bituminous coals in the first combustion stages of conventional and dry/wet oxy-combustion conditions (up to 10% vol. of H_2O). They found that fragmentation probability increased with H_2O concentration, both in air- and oxy-fired atmospheres, thus enhancing fuel reactivity.

* Corresponding author.
E-mail address: luisig@unizar.es (L.I. Díez).

https://doi.org/10.1016/j.energy.2023.128559
Received 17 November 2022; Received in revised form 5 May 2023; Accepted 25 July 2023
Available online 26 July 2023

Nomenclature

BET	Brunauer-Emmett-Teller
B	Biomass
C	Coal
c_p	Specific heat capacity (kJ/kmol K)
d	Diameter (m)
FC	Fixed carbon
TA	Torrefied agro-biomass
TP	Torrefied pine
VM	Volatile matter
α	Ash weight fraction, dry basis (−)
β	Burnout degree (%)
λ	Oxygen excess over stoichiometry (−)
ρ	Density (kg/m^3)

Several authors have found that adding biomass to coal in co-combustion leads to a reduction in NO_x emissions [4,24–26]. This is explained by a combination of factors [27,28], mainly related to the volatile and nitrogen contents in the biomass and to the larger NH_3/HCN ratios from biomass devolatilization. Riaza et al. [29] obtained a significant reduction of NO when replacing 10–20% of bituminous coal with olive waste, oxy-fired in an entrained flow reactor with 30–35% O_2. Skeen et al. [30] tested oxy-fuel combustion of sub-bituminous coal and sawdust, claiming that biomass particle size is influential on the NO_x formation rates under air-fired conditions but not under oxy-fired combustion.

To date, few studies have addressed the effect of steam addition on the NO emissions during biomass oxy-combustion. Moron et al. [31] researched NO_x emissions for different coals, biomasses (wood and straw) and blends in an entrained flow reactor, under different atmospheres: air and dry/wet oxy-combustion (up to 10% H_2O). They obtained a diminution of the NO emissions when H_2O is added, highlighting the role of CO in NO-to-N_2 reduction mechanisms. A similar result was reported by Jurado et al. [32], who conducted oxy-co-firing tests of different coal/biomass blends in a down-fired pulverized fuel burner, with H_2O up to 25% resembling wet recycling.

Concerning the oxy-fuel combustion of torrefied biomass, Panahi et al. [33] compared the air- and oxy-combustion characteristics of single particles from six torrefied biomasses, seeking O_2-optimization under dry conditions. Meng et al. [34] oxy-fired two raw and torrefied biomasses, observing significant increases of conversion rates and NO emissions when the atmosphere is enriched from 21/79% O_2/CO_2 to 30/70% O_2/CO_2. Tumsa et al. [35] compared the 30/70% O_2/CO_2 oxy-combustion of coal and torrefied palm kernel shell, relating the NO formation rates with the nitrogen and volatiles contents in the fuels.

As can be seen in the previous review, there is a limited knowledge about the combustion characteristics of biomass under oxy-combustion with large steam concentrations. Based on this, the present work aims to provide new experimental results encompassing burnout, combustion efficiency and NO formation. In particular, the study is focused on torrefied biomass, since the published experiences have been carried out only for dry atmospheres. To this purpose, comprehensive experimental campaigns have been carried out in an entrained flow reactor, with O_2 contents up to 35% and H_2O contents up to 40%. Although the experimental facility can be operated with higher oxygen concentrations, an upper limit of 35% O_2 has been selected, in accordance with the maximum values used in the largest demo-scale oxy-fired units so far [36].

2. Experiments

2.1. Fuels

Two pelletized biomasses of different origins were selected to proceed with torrefaction: 1) forestry residues from pine wood, and 2) agricultural residues from a mixture of 70% vineyard and 30% corn wastes. The pellets were torrefied in a lab-scale batch rotatory reactor, feeding N_2 during 70 min with a maximum temperature of 275 °C.

Table 1 summarizes the proximate and ultimate analysis of the raw and torrefied samples. The torrefaction degree achieved was 42.7% and 49.3% respectively, expressed as the fraction of the volatiles released during the torrefaction in comparison to the volatiles contained in the raw biomass (in dry basis). The main difference between the two biomasses is related to the ash content, which also influences the volatile to fixed carbon ratio (VM/FC). The nitrogen content is also significantly higher in the agricultural biomass than in the forestry one. In order to assess the effect of the biomass share during the tests, a medium-volatile bituminous coal (ASTM D388-97) was selected as a reference fossil fuel. Its analysis is also shown in Table 1. The proximate and ultimate analysis of the fuels were determined by a certified laboratory, belonging to the Spanish National Research Council. The equipment used to carry out the proximate analysis is a muffle furnace (Hobersal CRN-48), while the ultimate analysis is obtained by using a macro-analyzer LECO CHNS 628 and a micro-analyzer Thermo Flash 1112. The procedures accomplish the standards for each of the analysis: ISO 5068–2:2007, ISO 562:2010 and ISO 1171:2010 for the coal proximate analysis; ISO 18122:2016, ISO 18123:2016 and ISO 18134:2016 for the torrefied biomass proximate analysis; ISO 17247:2020 for the coal ultimate analysis; ISO 16948:2015 and ISO 16994:2016 for the torrefied biomass ultimate analysis.

All the fuels were grounded and sieved before the experiments: coal size within the range 75—150 μm while torrefied biomass size within 100—200 μm. These values were selected to get the same mean residence time (3 s) in the reactor; since the density of coal is higher, its size has to be lower to obtain comparable entrained conditions, as explained in section 2.3. Table 2 shows the particle size distribution for the three fuels (bituminous coal, torrefied pine and torrefied agricultural residues). The fuels were fired alone, but also two blends of 50% coal and 50% torrefied biomass (mass basis) were co-fired after being prepared in a rotary electromechanical mixer.

Table 1
Proximate and ultimate analysis of the fuels.

	Bituminous coal (C)	Pine wood (P)	Agricultural residues (A)	Torrefied pine wood (TP)	Torrefied agricultural residues (TA)
Proximate analysis (% wt.)					
Moisture	3.6	7.5	8.3	2.5	2.4
Ash	13.1	0.2	7.3	0.4	11.7
Volatile matter	25.9	76.8	69.4	68.6	50.8
Fixed carbon	57.4	15.5	15.0	28.5	35.1
VM/FC	0.45	4.95	4.63	2.41	1.45
Ultimate analysis (% wt., dry ash free)					
Carbon	82.22	52.13	51.51	60.43	67.02
Hydrogen	4.21	5.82	5.73	5.70	5.54
Nitrogen	2.04	0.10	0.72	0.16	1.11
Sulphur	0.51	0.02	0.02	0.02	0.02
Chlorine	0	0.02	0.14	0.02	0.18
Oxygen	11.02	41.91	41.88	33.66	26.13

Table 2
Particle size distribution of the fuels.

	Bituminous coal (C)	Torrefied pine wood (TP)	Torrefied agricultural residues (TA)
Mass fractions (%)			
<60 μm	1.1	0.4	0.5
60–80 μm	6.4	0.7	0.9
80–100 μm	20.9	1.5	1.8
100–120 μm	35.8	12.6	14.5
120–140 μm	24.1	19.1	21.9
140–160 μm	11.7	34.1	31.4
160–180 μm	0	24.2	23.1
180–200 μm	0	7.4	5.9

2.2. Experimental facility

The data and results presented in this paper were obtained from experiments developed in a lab-scale entrained flow reactor, shown in Fig. 1. The fuel feeding system consists of a hopper and an endless screw regulated by a variable-frequency motor. The gases feeding system consists of mass flow controllers that provide CO_2, O_2 and N_2 from bottles, while a Coriolis flowmeter controls the water flow rate. The reactor is a Kanthal APM tube of 38 mm diameter and 2 m height, surrounded by four independent electric furnaces. The length of the reaction section can be modified by a removable sampling probe located at the bottom.

Downstream the reactor, a cyclone and a filter retain the solid residues, and an ice-cooled condenser removes most of the moisture in flue gases. A continuous emission monitoring system is connected to the process, providing the flue gas composition in this section: non-dispersive infrared sensors for NO, CO and CO_2, and a paramagnetic module for O_2. The accuracies of the instruments used for the on-line measurements in the reactor are listed in Table 3.

2.3. Test campaigns

Combustion and oxy-combustion tests were conducted under different conditions: 21/79% O_2/N_2 (resembling air), 21/79% O_2/CO_2 and 35/65% O_2/CO_2. With the aim of studying the effect of steam, different contents of CO_2 in the atmospheres were replaced by H_2O: 10, 25 and 40%. In total, 9 tests were accomplished for each fuel and blend with the same oxygen excess of 1.25.

All the experiments were carried out for the same reactor temperature, 1000 °C. The reactor is externally heated by means of four electrical furnaces, controlled by four independent thermocouples. Both the power consumptions and the temperatures of the furnaces were continuously measured and recorded by the data acquisition system. Before starting the tests, the reactor is heated-up to the prescribed temperature. Once achieved, fuel feeding starts and after a transient

Table 3
Accuracy of the instruments for on-line measurements.

Measurement	Accuracy
Feeding gases flow rate (O_2, CO_2, N_2)	±0.5%
Feeding water flow rate	±0.2%
Temperature	±2 °C
Pressure	±3 mbar
Flue gases composition (CO_2, CO, NO)	±1%
Flue gases composition (O_2)	±1.5%

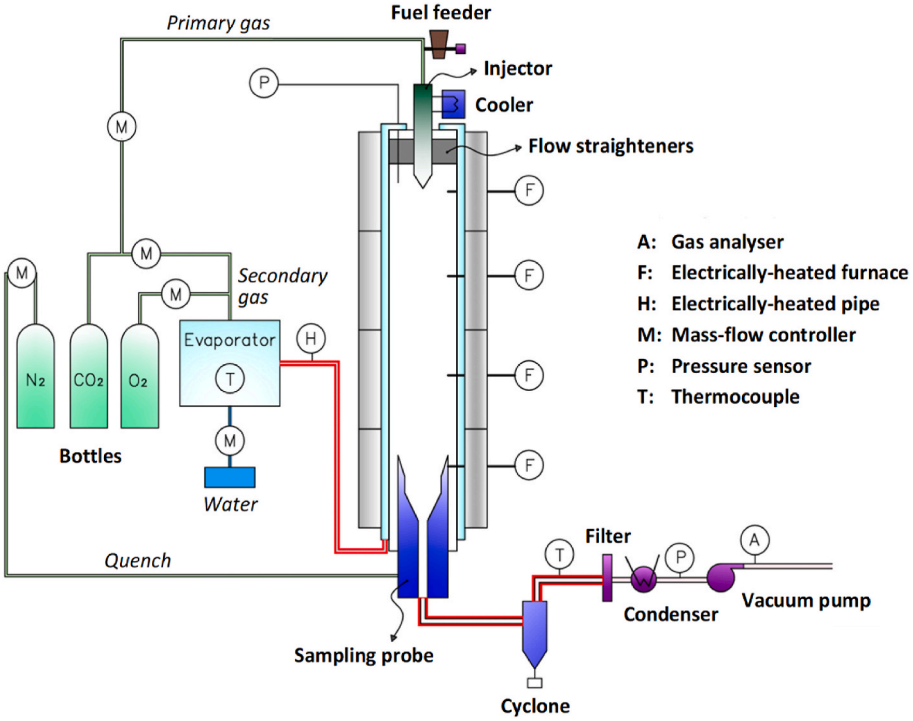

Fig. 1. Diagram of the lab-scale entrained flow reactor.

Table 4
Mass flow rates during the combustion tests of the 50% coal +50% torrefied biomass blends.

Atmosphere (% vol.)	Fuel flow rate (g/min)		O_2 flow rate (g/min)		CO_2 flow rate (g/min)		H_2O flow rate (g/min)	
	C + TP	C + TA	C + TP	C + TA	C + TP	C + TA	C + TP	C + TA
21/79 O_2/N_2	0.59	0.60	1.37	1.38	4.51 (N_2)	4.54 (N_2)	0	0
21/79 O_2/CO_2	0.59	0.60	1.37	1.38	7.07	7.13	0	0
21/69/10 $O_2/CO_2/H_2O$	0.59	0.60	1.37	1.38	6.18	6.22	0.37	0.37
21/54/25 $O_2/CO_2/H_2O$	0.59	0.60	1.37	1.38	4.84	4.87	0.92	0.93
21/39/40 $O_2/CO_2/H_2O$	0.59	0.60	1.37	1.38	3.49	3.52	1.47	1.48
35/65 O_2/CO_2	0.95	0.96	2.20	2.22	5.62	5.68	0	0
35/55/10 $O_2/CO_2/H_2O$	0.95	0.96	2.20	2.22	4.75	4.81	0.35	0.36
35/40/25 $O_2/CO_2/H_2O$	0.95	0.96	2.20	2.22	3.46	3.50	0.88	0.89
35/25/40 $O_2/CO_2/H_2O$	0.95	0.96	2.20	2.22	2.16	2.19	1.41	1.43

Table 5
Mass flow rates during the combustion tests of the 100% torrefied biomasses.

Atmosphere (% vol.)	Fuel flow rate (g/min)		O_2 flow rate (g/min)		CO_2 flow rate (g/min)		H_2O flow rate (g/min)	
	TP	TA	TP	TA	TP	TA	TP	TA
21/79 O_2/N_2	0.64	0.65	1.34	1.36	4.41 (N_2)	4.47 (N_2)	0	0
21/79 O_2/CO_2	0.64	0.65	1.34	1.36	6.92	7.03	0	0
21/69/10 $O_2/CO_2/H_2O$	0.64	0.65	1.34	1.36	6.05	6.14	0.36	0.36
21/54/25 $O_2/CO_2/H_2O$	0.64	0.65	1.34	1.36	4.73	4.80	0.90	0.91
21/39/40 $O_2/CO_2/H_2O$	0.64	0.65	1.34	1.36	3.42	3.47	1.43	1.46
35/65 O_2/CO_2	1.01	1.03	2.12	2.17	5.42	5.55	0	0
35/55/10 $O_2/CO_2/H_2O$	1.01	1.03	2.12	2.17	4.59	4.70	0.34	0.35
35/40/25 $O_2/CO_2/H_2O$	1.01	1.03	2.12	2.17	3.34	3.42	0.85	0.87
35/25/40 $O_2/CO_2/H_2O$	1.01	1.03	2.12	2.17	2.09	2.14	1.37	1.40

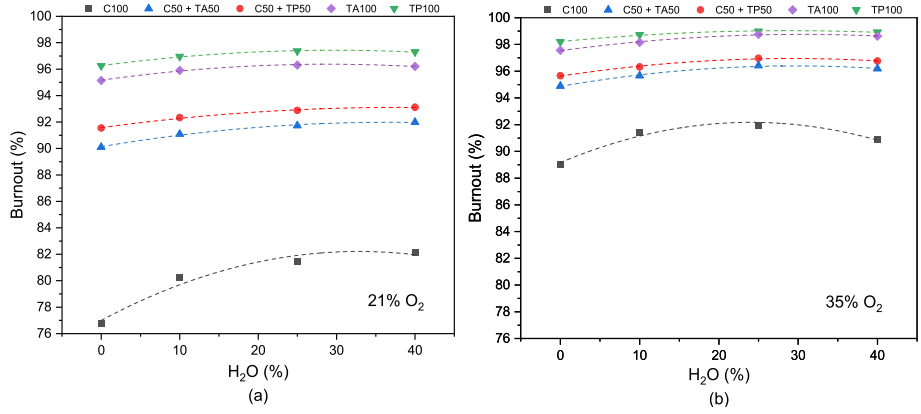

Fig. 2. Burnout degrees under O_2/CO_2 and $O_2/CO_2/H_2O$ atmospheres: effect of partial or full coal replacement by torrefied biomass. (a) 21% O_2, (b) 35% O_2.

period, the steady-state operation is accomplished. The steadiness is assessed by the composition of the flue gases at the reactor exit and the consumptions of the electrical furnaces. The on-line measurements gathered during the steady-state operation of every test enabled to calculate the fuel conversion rates to CO, CO_2 and NO. The mean values and standard deviations for each of these conversion rates, presented and discussed hereinafter in sections 3.2 and 3.3, have been obtained from at least 240 sets of operating data per fuel and atmosphere.

The mass flow rates of the entering gases were estimated to ensure a mean residence time of 3 s inside the reaction zone, which height was set to be 1.5 m. The mean residence time is calculated as the length of the reactor divided by the velocity of the mean-size particle. In an entrained flow reactor, the particle movement is due to a double contribution: 1) the vertical falling of a solid in a fluid, and 2) the drag effect caused by the supplied gases. The maximum particle velocity can be obtained as the sum of the terminal velocity and the gas velocity. Since the torrefied biomass density ρ_b is lower than the coal density ρ_c, the torrefied biomass particle diameter d_b has to be higher than the coal particle diameter d_c to get the same terminal velocity. According to Stokes' law (low Reynolds number), the following relation can be obtained:

$$\frac{d_b}{d_c} = \left(\frac{\rho_c}{\rho_b}\right)^{1/2} \quad (1)$$

Once the fuel type and size have been selected, and the same mean residence time is set, the mass flow rates of the supplied gases (N_2/O_2, CO_2/O_2, $CO_2/O_2/H_2O$) are calculated to get both the required atmosphere composition and the required gas velocity inside the reactor. Tables 4 and 5 summarize the mass flow rates used during the tests.

3. Results and discussion

3.1. Burnout

Fig. 2 shows the burnout rates obtained for the 21% O_2 and 35% O_2 cases, when firing coal alone, the two blends of coal and torrefied biomass, and the torrefied biomasses alone. The results corresponding to the 100% coal tests are already available in Escudero et al. [18], so here the focus is put on the results when torrefied biomass is partially or

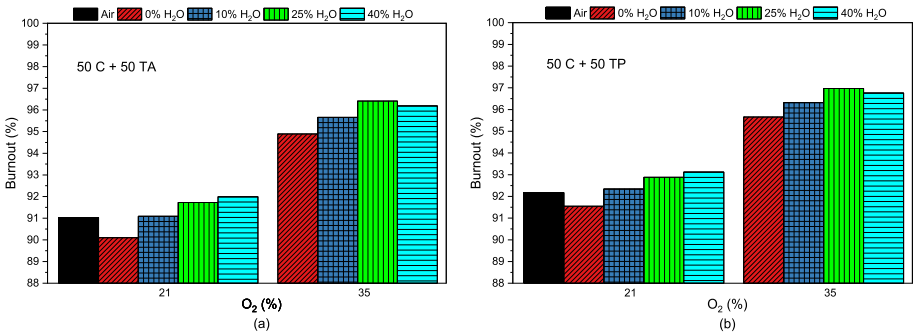

Fig. 3. Burnout degrees under O_2/N_2, O_2/CO_2 and $O_2/CO_2/H_2O$ atmospheres for 50% coal +50% torrefied biomass blends: effect of CO_2 replacement by H_2O. (a) 50 C + 50 TA, (b) 50 C + 50 TP.

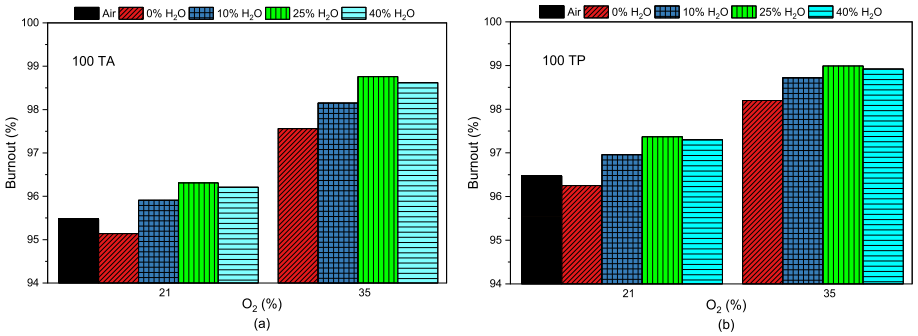

Fig. 4. Burnout degrees under O_2/N_2, O_2/CO_2 and $O_2/CO_2/H_2O$ atmospheres for 100% torrefied biomass: effect of CO_2 replacement by H_2O. (a) 100 TA, (b) 100 TP.

completely used as fuel. When coal is replaced by biomass, the burnout degrees are increased for all the cases. The larger volatile content is the main reason for this observation, but other factors also play a role: the higher char porosity and the catalytic effects caused by the alkalis bound in the biomass [24]. The burnout increase ranges 7.1−19.5 percentage points when torrefied pine fully replaces coal, while it ranges 6.8−18.4 percentage points when firing torrefied agro-biomass alone. The effect of O_2 enrichment from 21% to 35% is also clearly seen in Fig. 2. The larger O_2 availability increases flame temperature and volatile and char oxidation rates, leading to larger solid-to-gas conversion rates. Under dry conditions (0% H_2O), the differences between the two types of biomass are almost halved when shifting from 21% O_2 to 35% O_2: 1.45 and 0.77 percentage points respectively when 50% torrefied biomass co-firing, 1.11 and 0.64 percentage points when 100% torrefied biomass firing.

Fig. 3 displays the effect of replacing CO_2 by H_2O (10−40%) on the burnout of the two blends of 50% coal + 50% torrefied biomass. The trend is similar regardless the type of biomass used. For the 21% O_2 cases, the larger the steam content in the atmosphere, the higher the burnout degree: in comparison to the dry atmospheres, increases of 1.57 percentage points (50% TP) and 1.89 percentage points (50% TA) are obtained when replacing 40% CO_2 by H_2O. The trend is consistent with previous experiences [37] and explained by a twofold cause: firstly, the higher gas temperature due to the lower specific heat of H_2O in comparison to CO_2; secondly, the larger O_2 diffusivity in H_2O than in CO_2. Nevertheless, the increases of the burnout rates are not proportional to the steam contents, and some attenuation is observed for all the fuels. Indeed, for the 35% O_2 cases, the maximum burnout degrees are obtained for the 25% H_2O tests and not for the 40% ones. Steam increases char gasification in comparison to carbon dioxide, leading to a reduction of both the surrounding temperature and the internal specific surface [38,39]. Anyway, the addition of H_2O as CO_2 replacement always produces higher burnout rates in comparison to the dry atmospheres, for all the fuels and O_2 contents.

Fig. 4 displays the effect of replacing CO_2 by H_2O in the burnout when the torrefied biomasses are fired alone. In this case, the maximum conversions are always obtained for the 25% H_2O concentrations, both in the 21% and 35% O_2 tests. As reported by Zhijun et al. [40], the steam concentration leading to maximum conversions and minimum emissions depends on the fuel rank, i.e. the VM/FC ratio. This can be related to the effects on the char specific surfaces produced by the steam in comparison to carbon dioxide. To confirm this, the BET surfaces of a selection of samples taken from the cyclone were determined by N_2 isothermal adsorption at 77 K. These samples were previously degassed (250 °C, 5 h). In the case of the residues from the 100% TP tests, the reduction obtained in BET char surface was 28.1%: 333.4 m^2/g (21/79% O_2/CO_2) vs. 239.7 m^2/g (21/39/40% $O_2/CO_2/H_2O$). In the case of the residues from the 100% TA tests, the reduction was 26.5%: 301.2 m^2/g (21/79% O_2/CO_2) vs. 221.4 m^2/g (21/39/40% $O_2/CO_2/H_2O$).

All the burnout degrees depicted in Figs. 3 and 4 represent the mean values obtained from a pair of solid samples taken for every experimental condition. Relative standard deviations are not represented in the figures since they are similar and very small, below 0.15% of the mean values for all the tests.

The results for the 21/79% O_2/N_2 tests are also represented in Figs. 3 and 4, in order to assess the values obtained for oxy-combustion in comparison to conventional air combustion. It is well-known that switching from 21/79% O_2/N_2 to 21/79% O_2/CO_2 reduces the flame temperature ($c_{p,N2} < c_{p,CO2}$) and then lower conversions are obtained. This can be compensated in oxy-combustion by enriching the O_2 concentration: all the burnouts obtained in the tests for the 35% O_2 atmospheres are over the obtained for the atmospheres resembling air.

3.2. C-fuel conversion to CO and CO_2

Burnout represents the solid-to-gas conversion ratio, but additional information is required to seek the combustion efficiency, that is the homogeneous conversion to final products in the gas-phase. To this purpose, CO and CO_2 concentration in flue gases was used to discuss the effect of the torrefied biomass type and share on the blend, as well as the

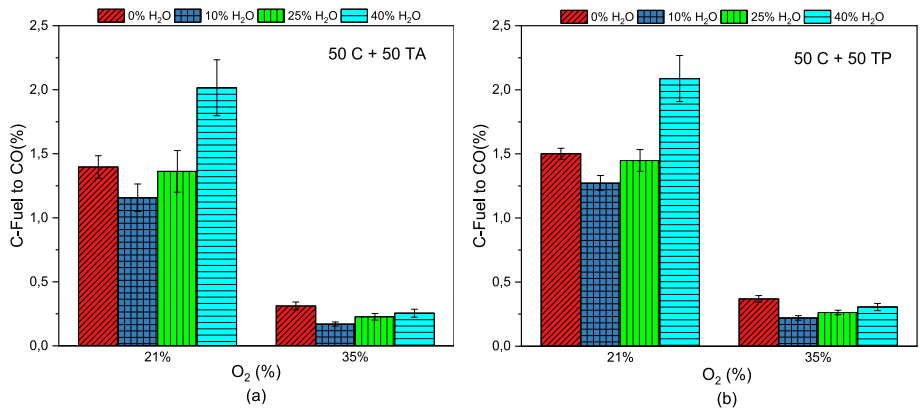

Fig. 5. C-fuel to CO conversions under O_2/CO_2 and $O_2/CO_2/H_2O$ atmospheres for 50% coal +50% torrefied biomass blends: effect of CO_2 replacement by H_2O. (a) 50 C + 50 TA, (b) 50 C + 50 TP.

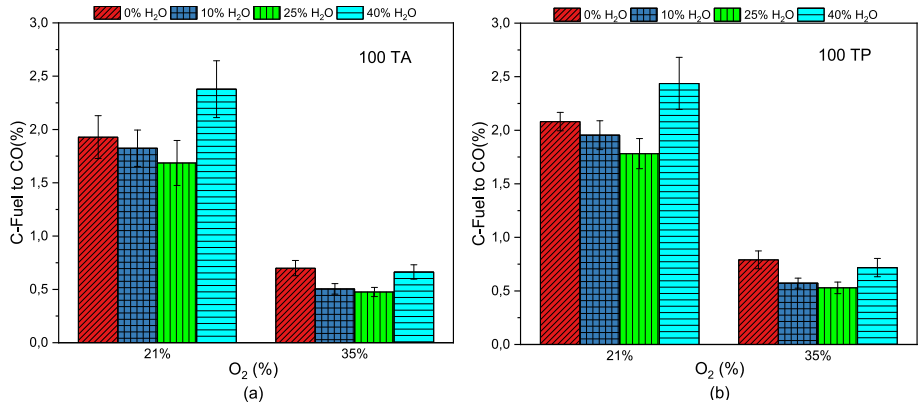

Fig. 6. C-fuel to CO conversions under O_2/CO_2 and $O_2/CO_2/H_2O$ atmospheres for 100% torrefied biomass: effect of CO_2 replacement by H_2O. (a) 100 TA, (b) 100 TP.

O_2 and H_2O concentration, on the combustion efficiency. C-fuel conversions to CO and CO_2 are determined from the following available information during the experiments: fuel flow rate supplied to the reactor, carbon content in the fuel (ultimate analysis), CO and CO_2 concentration in the flue gases provided by the gas analyzer. Carbon mass balance can be then closed, and the mass conversion rates can be calculated.

As concerns the uncertainty linked to the calculation of the C-fuel conversion to CO and CO_2, they mainly rely on the accuracy of the gas analyzer –reported in Table 3– and the uncertainty of the fuel mass flow rate. The fuel flow rate is not directly measured during the tests, but the frequency of the motor driving the endless screw is. Previously to the tests, the frequency is correlated to the mass flow rate for every fuel and blend, by the discharge calibration of the endless screw. Anyway, the error of the fuel flow rates can be assessed by the closure of the overall mass balance, since the fuel composition, the burnout degree and the flue gas composition are known for every experimental test. The deviations of the fuel flow rates, between the expected and the actual ones, have been comprised within the range 1.9–3.1%. Assuming that this uncertainty is independent and not correlated to the accuracy of the gas analyzer, the uncertainties propagation has been computed resulting in ±2.2−3.3% for the C-fuel conversion rates. The same range applies to

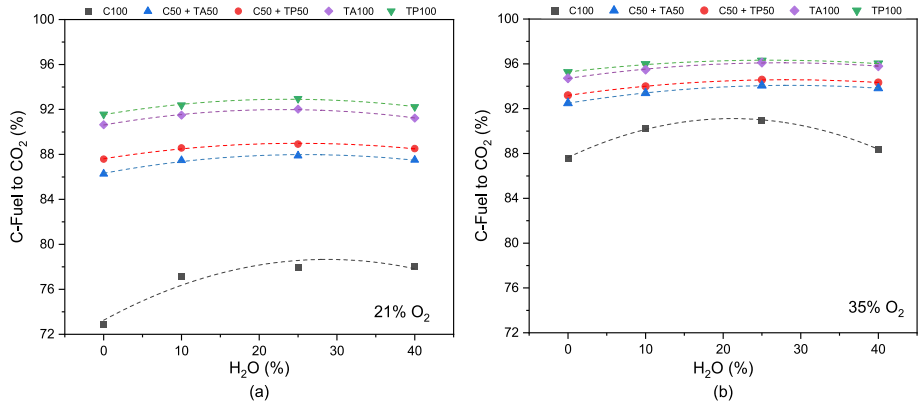

Fig. 7. C-fuel to CO_2 conversions under O_2/CO_2 and $O_2/CO_2/H_2O$ atmospheres: effect of partial or full coal replacement by torrefied biomass. (a) 21% O_2, (b) 35% O_2.

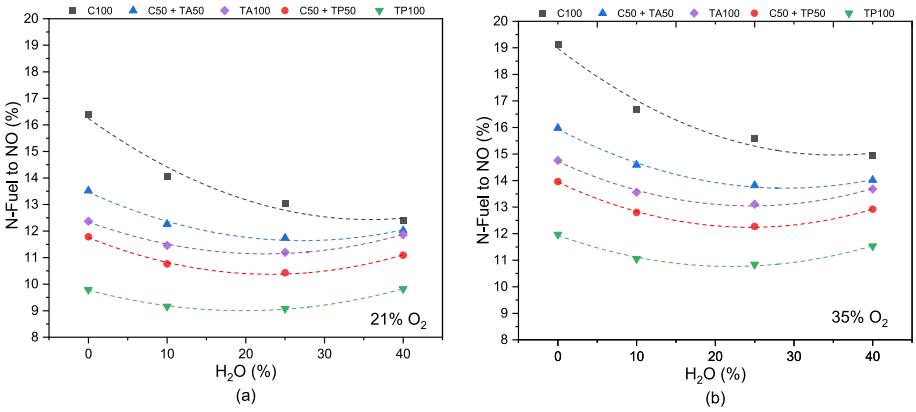

Fig. 8. N-fuel to NO conversions under O_2/CO_2 and $O_2/CO_2/H_2O$ atmospheres: effect of partial or full coal replacement by torrefied biomass. (a) 21% O_2, (b) 35% O_2.

the calculation of the N-fuel to NO conversion rate discussed in section 3.3.

Figs. 5 and 6 depict the C-fuel conversion to CO (mean values and standard deviations), for all the fuels fired and the atmospheres tested. Relative standard deviations are within the range 2.86–10.94% of the mean values. The effect of O_2 enrichment is a clear diminution of the CO levels at the reactor exit; for the 35% O_2 cases, conversions are always below 0.4% for the blends, and below 0.8% for the torrefied biomasses. The larger oxygen availability enhances the CO oxidation to CO_2 in the gas phase, explaining the significant reductions observed. For every particular atmosphere, the use of torrefied pine slightly increases CO in comparison to torrefied agro-biomass. This is consistent with the burnout rates presented in the previous section, and related to the higher reactivity of the torrefied pine biomass with great volatile content and almost negligible content in ash.

The effect of replacing CO_2 by H_2O is very similar for all the blends and torrefied biomasses. When 10% H_2O is added, a diminution of CO is always obtained in comparison to the dry atmospheres, both for 21% O_2 and 35% O_2. The higher O_2 diffusivity in H_2O explains those results. Nevertheless, the trend is reversed when the H_2O concentration is raised to 40%. Even, for the 21/40% O_2/H_2O cases the CO concentration is higher than the 21/0% O_2/H_2O ones. The intensification of char gasification due to the steam addition enhances C-char heterogeneous conversion to CO that cannot be compensated before quenching the CO oxidation to CO_2 at the reactor exit. The gasification rates are lowered for the 35% O_2 cases, due to the larger O_2 content [38].

In any case, the C-fuel conversions to CO are low for all the experiments; for this reason, the mean values of the C-fuel conversion to CO_2 in Fig. 7 follow a very similar trend to that previously presented for the burnouts in Fig. 2. Relative standard deviations, not represented in Fig. 7 for the sake of clarity, are within the range 0.17–2.44% of the mean values. CO concentrations are not high enough to modify the main conclusions already obtained in section 3.1: a) coal replacement by torrefied biomass increases the combustion efficiency, b) feeding torrefied pine results in slightly higher conversions than torrefied agro-biomass, c) the larger the O_2 concentration, the larger the combustion efficiency, d) CO_2 replacement by H_2O in the firing atmosphere results in a concentration maximizing the efficiency due to overlapped, opposite tendencies (increase of temperature and O_2 diffusivity vs. decrease of char specific surfaces).

3.3. N-fuel conversion to NO

During oxy-combustion of solid fuels, in the absence of N_2, nitric oxide (NO) is the main nitrogen oxide formed, coming from the nitrogen bound in the fuel (which is known as "fuel-NO_x"). Fig. 8 shows the effect of partially or fully replacing coal by torrefied biomass on the N-fuel conversion to NO. The use of torrefied biomass diminishes the NO formation to a significant extent. In the case of firing the blends, maximum reductions are 17.6% (50 C + 50 TA) and 28.1% (50 C + 50 TP). In the case of firing the torrefied biomasses alone, maximum reductions are 24.6% (100 TA) and 40.3% (100 TP). These reductions are related to the mass conversions of nitrogen, not meaning a reduction in emissions (i.e. NO concentration in flue gases). Since the nitrogen bound in the torrefied biomasses is lower than the bound in the coal (as shown in Table 1), the reductions in terms of NO emissions will be higher than those shown in Fig. 8.

Two intermediate compounds from fuel devolatilization, HCN and NH_3, are the main precursors of fuel-NO_x. Differently from high- and mid-rank coals, NH_3 is the predominant species released from biomass conversion [41]. NH_3 can be partially oxidized to NO, but also can contribute to NO depletion for temperatures over 900 °C [42,43]:

$$NH_3 + NO + \frac{1}{4}\,O_2 \rightarrow N_2 + \frac{3}{2}\,H_2O \quad \text{(R.1)}$$

$$NH_3 + \frac{3}{2}\,NO \rightarrow \frac{5}{4}\,N_2 + \frac{3}{2}\,H_2O \quad \text{(R.2)}$$

N-char oxidation also contributes to some NO formation, which is lower in the case of the torrefied biomasses accordingly to their higher VM/FC ratio. Moreover, a fraction of N-char can be directly converted to NH_3 in the presence of H_2O [44], which after competitively participates in oxidation/reduction mechanisms.

The use of torrefied pine yields larger NO reductions than the use of torrefied agro-biomass (Fig. 8). Besides the much lower nitrogen content in the torrefied pine, the largest volatile content also can play a role. Light hydrocarbon radicals from devolatilization contribute to NO depletion, in a similar way to the "reburning" technique used for NO_x control [45].

The effect of O_2-enrichment is clearly seen in Fig. 8: NO formation is increased to a significant extent for all the fuels, since O_2 partial pressure is the most influential variable in the fuel-NO_x mechanism. In the case of firing the blends, maximum increases are of 18.8% (50 C + 50 TA) and 19.2% (50 C + 50 TP). In the case of firing the torrefied biomasses alone, the maximum increases are 19.6% (100 TA) and 22.3% (100 TP).

Steam is known to contribute to NO_x reduction through several mechanisms, which have been studied for both conventional and oxy-combustion conditions. On the one hand, H_2O can participate in homogeneous reactions in the gas-phase, either by directly reacting with HCN over 600 °C (R.3) [46] or through the participation of H + OH radicals (R.4, R.5) [47]:

$$HCN + H_2O \rightarrow NH_3 + CO \quad \text{(R.3)}$$

$$HCN + H \leftrightarrow H_2 + CN \quad \text{(R.4)}$$

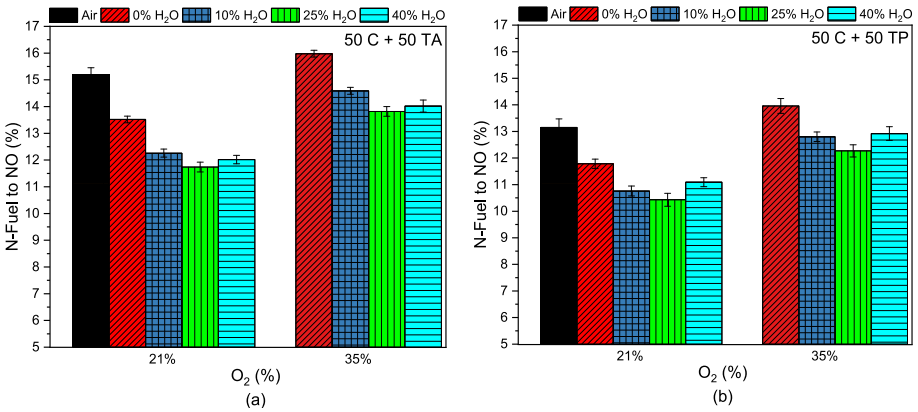

Fig. 9. N-fuel to NO conversions under O_2/CO_2 and $O_2/CO_2/H_2O$ atmospheres for 50% coal +50% torrefied biomass blends: effect of CO_2 replacement by H_2O. (a) 50 C + 50 TA, (b) 50 C + 50 TP.

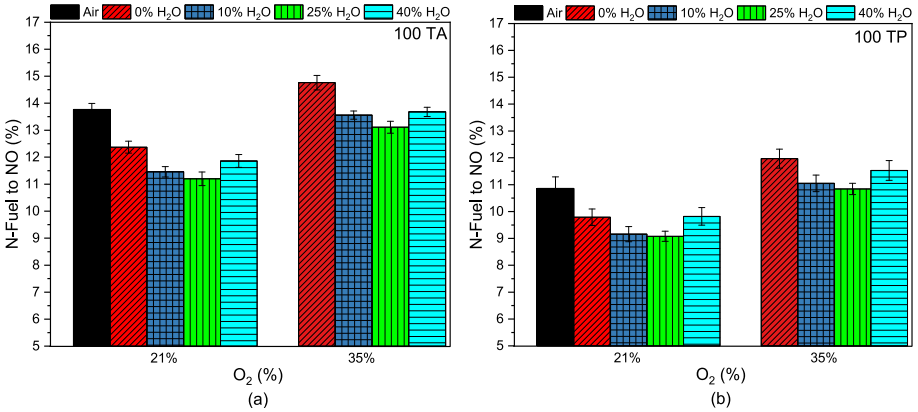

Fig. 10. N-fuel to NO conversions under O_2/CO_2 and $O_2/CO_2/H_2O$ atmospheres for 100% torrefied biomass: effect of CO_2 replacement by H_2O. (a) 100 TA, (b) 100 TP.

$$HCN + OH \leftrightarrow H_2O + CN \quad (R.5)$$

The set of reactions (R.3), (R.4) and (R.5) compete with HCN oxidation, thus reducing the NO formation rates. NH_3 from reaction (R.3) can further contribute to the NO reduction to N_2 by means of the reactions (R.1) and (R.2).

On the other hand, steam also intensifies char gasification, releasing CO that can additionally reduce NO by the reaction (R.6) catalyzed by the char surface [48]. Moreover, char gasification also results in carbon-free sites on the solid surface, participating in a heterogeneous reduction of NO in the solid proximity (R.7) [49]:

$$CO + NO \rightarrow \frac{1}{2} N_2 + CO_2 \quad (R.6)$$

$$C(s) + NO \rightarrow \frac{1}{2} N_2 + CO \quad (R.7)$$

The set of equations (R.3)−(R.7) summarizes the main mechanisms contributing to NO reduction due to H_2O, during combustion and oxy-combustion of solid fuels. Nevertheless, when large amounts of steam are present, other effects have to be accounted for. In the absence of N_2, fuel-NO_x is the main route for NO_x formation, that is strongly dependent on O_2 concentration. Since O_2 diffusivity in H_2O is higher than in CO_2, the oxidation rates are increased, also influenced by the higher flame temperature under $O_2/CO_2/H_2O$ atmospheres in comparison to O_2/CO_2 ones. Besides, the larger availability of OH radicals can deplete CO according to reaction (R.8), then limiting the extent of the reaction (R.6):

$$CO + OH \rightarrow CO_2 + H \quad (R.8)$$

The effect of CO_2 replacement by H_2O on the conversion of N-fuel to NO is shown in more detail in Fig. 9, for the two blends of coal and torrefied biomass, and the conditions given in Table 4: two O_2 concentrations (21%, 35%), four steam concentrations (0%, 10%, 25%, 40%) and oxygen excess = 1.25. Mean values and standard deviations are represented in Fig. 9; relative standard deviations are within the range 0.79–2.34% of the mean values. The trend obtained is very similar for both blends. When 10% CO_2 is replaced by H_2O a clear reduction of NO is observed in comparison to the dry atmosphere: 9.3% and 8.7% in the case of the blend with torrefied agro-biomass, 8.6% and 8.3% in the case of the blend with torrefied pine. The reducing mechanisms described hereinbefore explain this behaviour, which is consistent with other experiences [43].

NO is further reduced when 25% CO_2 is replaced by H_2O, but not proportionally to the steam content: 13.1% and 13.5% in the case of the blend with torrefied agro-biomass, 11.5% and 12.1% in the case of the blend with torrefied pine, all of them in relation to the dry atmospheres. Thus, a clear attenuation is observed, the reduction is more relevant from 0% to 10% than from 10% to 25%. When H_2O concentration is raised up to 40% the trend is reversed for the two blends and the two O_2 contents. This behaviour has been also observed by Zhijun et al. [40], pointing out that large CO_2 replacements by H_2O contribute to a fuel-NO_x intensification.

Fig. 10 shows the effect of CO_2 replacement by H_2O on the conversion of N-fuel to NO, when oxy-firing torrefied biomass alone. For these tests, relative standard deviations are within the range 1.13–3.32% of the mean values. The effect of steam addition is very similar to the

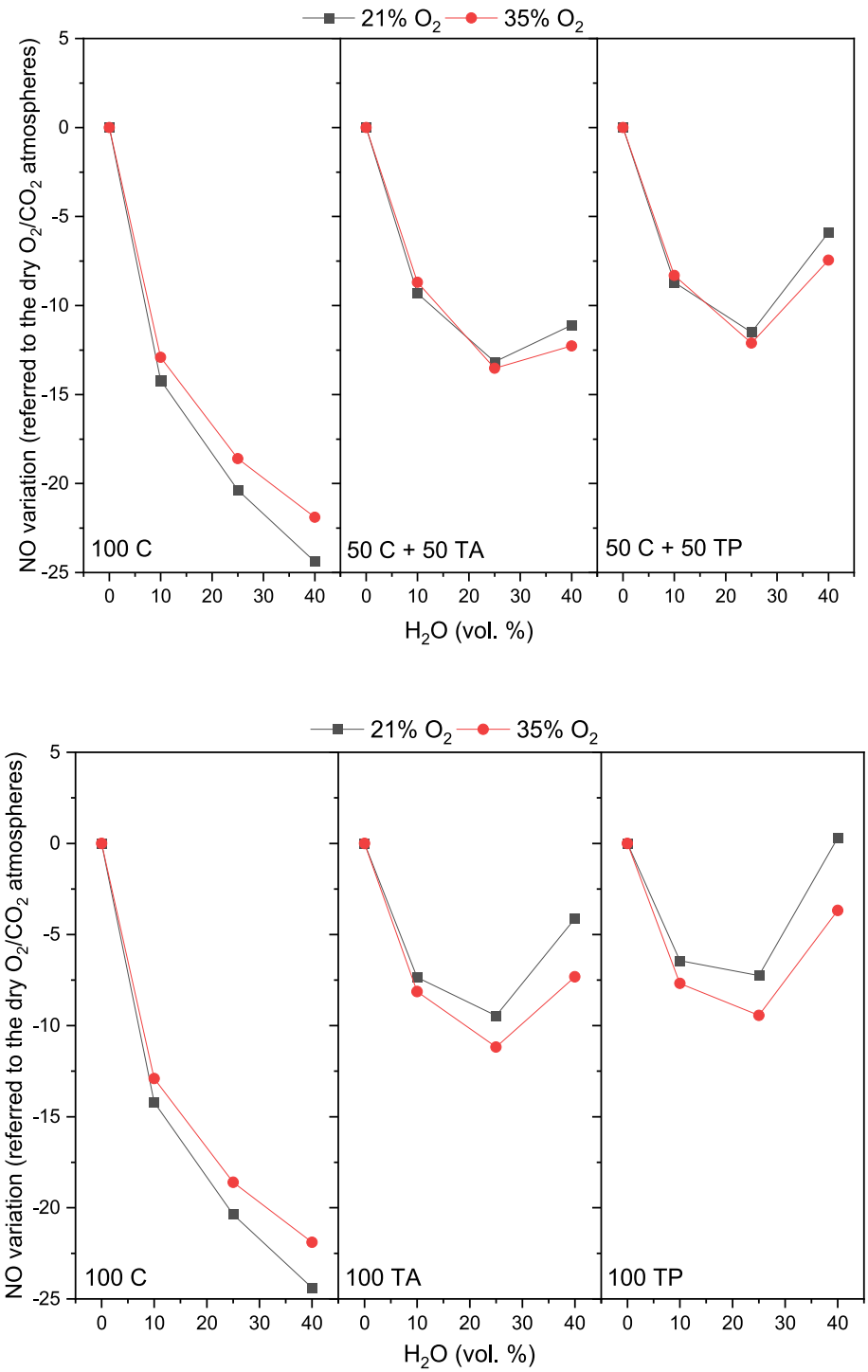

Fig. 11. Accumulative variations (%) in fuel-N to NO conversion rates for different H_2O concentrations: 100% coal, blends of 50% coal + 50% torrefied biomass, 100% torrefied biomass. Results corresponding to 100% coal tests can be found in Ref. [18].

observed for the coal + torrefied biomass blends, and the minimum conversions are always detected for the 25% H_2O cases. In comparison to the dry atmospheres, the maximum NO reductions observed are 9.5% and 11.2% for the torrefied agro-biomass, and 7.2% and 9.4% for the torrefied pine.

In order to better see the different extent of steam influence on NO reduction depending on the fuel rank, Fig. 11 compares the accumulative variations of fuel-N to NO conversion rates for 100% coal, blends of 50% coal +50% torrefied biomasses, and 100% torrefied biomasses. As seen in Fig. 11, the lower the fuel rank (i.e. the higher the VM/FC ratio), the lower the reducing effect caused by the H_2O. Indeed, for the experiments with 100% torrefied pine —the fuel with the higher VM/CF ratio—, two results worth to be mentioned: 1) there are small differences in NO levels between 10% and 25% H_2O tests, 2) a slight increase (0.3%) of NO is obtained for the 21/40% O_2/H_2O test in comparison to the dry atmosphere. The larger release of NO_x precursors during devolatilization, along with their oxidation due to the increased O_2 diffusivity and gas-phase temperature, are more influential than the reducing mechanisms in which steam is involved. Therefore, whether compared to coal, the $\%H_2O$ resulting in minimum NO levels is reduced.

4. Conclusions

The oxy-combustion characteristics of two torrefied biomasses, fired alone and co-fired with coal, have been determined in a lab-scale entrained flow reactor. A set of 9 experiments has been conducted for each biomass and blend, under a combination of O_2/N_2, O_2/CO_2 and $O_2/CO_2/H_2O$ atmospheres. Two oxygen concentrations (21%, 35%) and four steam concentrations (0%, 10%, 25%, 40%) are selected, steam acting as CO_2 replacement. The insights obtained from the experimental campaigns are the following:

- Partial (50%) or full (100%) replacement of coal by torrefied biomass always increases the solid-to-gas conversion rates (burnout), mainly due to their larger VM/FC ratios. The use of torrefied pine results in better conversions than torrefied agro-biomass, but the differences are very low when the atmospheres are O_2-enriched up to 35%. The 40% H_2O cases show the largest CO peaks due to the intensification of char gasification caused by the steam.
- Partial (50%) or full (100%) replacement of coal by torrefied biomass always decreases the N-fuel to NO formation rates. The use of torrefied pine provides more reductions than the agro-biomass, and the O_2-enrichment of the firing atmosphere significantly increases the N-fuel oxidation rates.
- Burnout degrees of the torrefied biomasses, co-fired or fired alone, are increased when H_2O replaces CO_2 in the atmosphere. Nevertheless, in most situations, the maximum steam concentration (40%) does not yield the maximum conversion rates. The effect of steam on reducing the char specific surface is opposed to the increase of temperature and O_2 diffusivity, and maximum conversions are detected for the 25% H_2O tests.
- The extent of the NO reduction due to CO_2 replacement by H_2O depends on the fuel rank and the H_2O concentration. Regardless the torrefied biomass type and share, NO levels are minimum for the 25% H_2O cases. The observed trends are explained by the opposite, overlapped effects caused by the steam addition: homogeneous and heterogeneous NO reductions, either directly or by means of competitive pathways, vs intensification of the N-fuel oxidation. The lower the fuel rank, the lower the extent of the NO diminution due to the CO_2 replacement by H_2O.

Concluding, O_2/CO_2 and $O_2/CO_2/H_2O$ combustion of torrefied biomasses presents better behaviour than coal. Within the values tested in this work, the replacement of 25% CO_2 by H_2O results in the maximization of conversion and minimization of NO for most of the cases. Oxy-combustion offers a particular potential for agro-biomasses due to the flexibility in establishing an adequate O_2 concentration. Nevertheless, other issues should be also evaluated, like fouling and corrosion risks due to the ashes composition, which could represent a limitation for the use of torrefied biomass and blends in oxy-fired systems.

Declaration of competing interest

The authors declare that they have no known competing financial interests or personal relationships that could have appeared to influence the work reported in this paper.

Data availability

Data will be made available on request.

Acknowledgements

The work described in this paper has been co-funded by the National Research Program from the Spanish Ministry of Science and Innovation, under the Project RTI2018-094488, and the European Funds for Regional Development.

References

[1] Baxter L. Biomass-coal co-combustion: opportunity for affordable renewable energy. Fuel 2005;84:1295–302. https://doi.org/10.1016/j.fuel.2004.09.023.
[2] Tillman DA. Biomass cofiring: the technology, the experience, the combustion consequences. Biomass Bioenergy 2000;19:365–84. https://doi.org/10.1016/S0961-9534(00)00049-0.
[3] Li R, Kai X, Yang T, Sun Y, He Y, Shen S. Release and transformation of alkali metals during co-combustion of coal and sulfur-rich wheat straw. Energy Convers Manag 2014;83:197–202. https://doi.org/10.1016/j.enconman.2014.02.059.
[4] Wang X, Tan H, Niu Y, Pourkashanian M, Ma L, Chen E, Liu Y, Liu Z, Xu T. Experimental investigation on biomass co-firing in a 300 MW pulverized coal-fired utility furnace in China. Proc Combust Inst 2011;33:2725–33. https://doi.org/10.1016/j.proci.2010.06.055.
[5] Demirbas A. Potential applications of renewable energy sources, biomass combustion problems in boiler power systems and combustion related environmental issues. Prog Energy Combust Sci 2005;31:171–92. https://doi.org/10.1016/j.pecs.2005.02.002.
[6] Sher F, Yaqoob A, Saeed F, Zhang S, Jahan Z, Klemes JJ. Torrefied biomass fuels as a renewable alternative to coal in co-firing for power generation. Energy 2020;209:118444. https://doi.org/10.1016/j.energy.2020.118444.
[7] Arasto A, Onarheim K, Tsupari E, Karki J, Bio-CCS. Feasibility comparison of large scale carbon-negative solutions. Energy Proc 2014;63:6756–69. https://doi.org/10.1016/j.egypro.2014.11.711.
[8] Komaki A, Gotou T, Uchida T, Yamada T, Kiga T, Spero C. Operation experiences of oxyfuel power plant in Callide oxyfuel project. Energy Proc 2014;63:490–6. https://doi.org/10.1016/j.egypro.2014.11.053.
[9] Yin C, Yan J. Oxy-fuel combustion of pulverized fuels: combustion fundamentals and modeling. Appl Energy 2016;162:742–62. https://doi.org/10.1016/j.apenergy.2015.10.149.
[10] Salvador C, Mitrovi M, Zanganeh K. Novel oxy-steam burner for zero-emission power plants. 1st OCC, IEAGHG; 2009.
[11] Seepana S, Jayanti S. Steam-moderated oxy-fuel combustion. Energy Convers Manag 2010;51:1981. https://doi.org/10.1016/j.enconman.2010.02.031. –1988.
[12] Wall T, et al. An overview on oxyfuel coal combustion – state of the art research and technology development. Chem Eng Res Des 2009;87:1003–106. https://doi.org/10.1016/j.cherd.2009.02.005.
[13] Scheffknecht G, Al-Makhadmeh L, Schnell U, Maier J. Oxy-fuel coal combustion – a review of the current state-of-the-art. Int J Greenh Gas Control 2011;55:S16–35. https://doi.org/10.1016/j.ijggc.2011.05.020.
[14] Zou C, Cai L, Wu D, Liu Y, Liu S, Zheng C. Ignition behaviours of pulverized coal particles in O_2/N_2 and O_2/H_2O mixtures in a drop tube furnace using flame monitoring techniques. Proc Combust Inst 2015;35:3629–36. https://doi.org/10.1016/j.proci.2014.06.067.
[15] Hao Z, Li Y, Li N, Cen K. Experimental investigation of ignition and combustion characteristics of single coal and biomass particles in O_2/N_2 and O_2/H_2O. J Energy Inst 2019;92:502–11. https://doi.org/10.1016/j.joei.2018.04.008.
[16] Kops RB, Pereira FM, Rabaçal M, Costa M. Effect of steam on the single particle ignition of solid fuels in a drop tube furnace under air and simulated oxy-fuel conditions. Proc Combust Inst 2019;37:2977–85. https://doi.org/10.1016/j.proci.2018.05.091.
[17] Escudero AI, Aznar M, Díez LI, Mayoral MC, Andrés JM. From O_2/CO_2 to O_2/H_2O combustion: the effect of large steam addition on anthracite ignition, burnout and NOx formation. Fuel Process Technol 2020;206:106432. https://doi.org/10.1016/j.fuproc.2020.106432.
[18] Escudero AI, Aznar M, Díez LI. Oxy-steam combustion: the effect of coal rank and steam concentration on combustion characteristics. Fuel 2021;285:119218. https://doi.org/10.1016/j.fuel.2020.119218.
[19] Bai C, Zhang W, Deng L, Zhao Y, Sun S, Feng D, Wu J. Experimental study of nitrogen conversion during char combustion under a pressurized O_2/H_2O atmosphere. Fuel 2022;311:122529. https://doi.org/10.1016/j.fuel.2021.122529.
[20] Deng L, Zhao Y, Sun S, Feng D, Zhang W. Review on thermal conversion characteristics of coal in O_2/H_2O atmosphere. Fuel Process Technol 2022;232:107266. https://doi.org/10.1016/j.fuproc.2022.107266.
[21] Gil MV, Riaza J, Álvarez L, Pevida C, Pis JJ, Rubiera F. A study of oxy-coal combustion with steam addition and biomass blending by thermogravimetric analysis. J Therm Anal Calorim 2012;109:49–55. https://doi.org/10.1007/s10973-011-1342-y.
[22] Lei K, Zhang R, Ye B, Cao J, Liu D. Combustion of single particles from sewage sludge/pine sawdust and sewage sludge/bituminous coal under oxy-fuel conditions with steam addition. Waste Manag 2020;101:1–8. https://doi.org/10.1016/j.wasman.2019.09.034.
[23] Rabaçal M, Kops RB, Pereira FM, Costa M. Direct observations of single particle fragmentation in the early stages of combustion under dry and wet conventional and oxy-fuel conditions. Proc Combust Inst 2019;37:3005–12. https://doi.org/10.1016/j.proci.2018.07.001.
[24] Munir S, Nimmo W, Gibbs BM. The effect of air staged, co-combustion of pulverised coal and biomass blends on NO_x emissions and combustion efficiency. Fuel 2011;90:126–35. https://doi.org/10.1016/j.fuel.2010.07.052.
[25] Wei X, et al. Detailed modeling of NO_x and SO_x formation in co-combustion of coal and biomass with reduced kinetics. Energy Fuel 2012;26:3117–24. https://doi.org/10.1021/ef201729r.
[26] Daood SS, Javed MT, Gibbs BM, Nimmo W. NO_x control in coal combustion by combining biomass cofiring, oxygen enrichment and SNCR. Fuel 2013;105:283–92. https://doi.org/10.1016/j.fuel.2012.06.087.

[27] Thanapal SS, Annamalai K, Ansley RJ, Ranjan D. Co-firing carbon dioxide-torrefied woody biomass with coal on emission characteristics. Biomass Convers. Biorefinery 2016;6:91–104. https://doi.org/10.1007/s13399-015-0166-6.
[28] Karlström O, Perander M, DeMartini N, Brink A, Hupa M. Role of ash on the NO formation during char oxidation of biomass. Fuel 2017;190:274–80. https://doi.org/10.1016/j.fuel.2016.11.013.
[29] Riaza J, Gil MV, Álvarez L, Pevida C, Pis JJ, Rubiera F. Oxy-fuel combustion of coal and biomass blends. Energy 2012;41:429–35. https://doi.org/10.1016/j.energy.2012.02.057.
[30] Skeen SA, Kumfer BM, Axelbaum RL. Nitric oxide emissions during coal and coal/biomass combustion under air-fired and oxy-fuel conditions. Energy Fuel 2010;24:4144–52. https://doi.org/10.1021/ef100299n.
[31] Moroń W, Rybak W. NO_x and SO_2 emissions of coals, biomass and their blends under different oxy-fuel atmospheres, Atmos. Environ Times 2015;116:65–71. https://doi.org/10.1016/j.atmosenv.2015.06.013.
[32] Jurado N, Simms NJ, Anthony EJ, Oakey JE. Effect of co-firing coal and biomass blends on the gaseous environments and ash deposition during pilot-scale oxy-combustion trials. Fuel 2017;197:145–58. https://doi.org/10.1016/j.fuel.2017.01.111.
[33] Panahi A, Toole N, Wang X, Levendis YA. On the minimum oxygen requirements for oxy-combustion of single particles of torrefied biomass. Combust Flame 2020;213:426–40. https://doi.org/10.1016/j.combustflame.2019.12.012.
[34] Meng X, Rokni E, Zhou W, Qi H, Sun R, Levendis YA. Emissions from oxy-combustion of raw and torrefied biomass. J Energy Resour Technol 2020;142:122307. https://doi.org/10.1115/1.4047330.
[35] Tumsa TZ, Chae TY, Yang W, Paneru M, Maier J. Experimental study on combustion of torrefied palm kernel shell (PKS) in oxy-fuel environment. Int J Energy Res 2019;43:7508–16. https://doi.org/10.1002/er.4792.
[36] Lockwood T. Developments in oxy-fuel combustion of coal. IEA Clean Coal Centre; August 2014. 978–92–9029–561-7.
[37] Riaza J, Álvarez L, Gil MV, Pevida C, Pis JJ, Rubiera F. Effect of oxy-fuel combustion with steam addition on coal ignition and burnout in an entrained flow reactor. Energy 2011;36:5314–9. https://doi.org/10.1016/j.energy.2011.06.039.
[38] Hecht ES, Shaddix CR, Geier M, Molina A, Haynes BS. Effect of CO_2 and steam gasification reactions on the oxy-combustion of pulverized coal char. Combust Flame 2012;159:3437–47. https://doi.org/10.1016/j.combustflame.2012.06.009.
[39] Xu J, Su S, Sun Z, Si N, Qing M, Liu L, Hu S, Wang Y, Xiang J. Effects of H_2O gasification reaction on the characteristics of chars under oxy-fuel combustion conditions with wet recycle. Energy Fuel 2016;30:9071–9. https://doi.org/10.1021/acs.energyfuels.6b01725.
[40] Zhijun S, Su S, Xu J, Xu K, Hu S, Wang Y, Jiang L, Si N, Zhou Y, Syed-Hassan SSA, Zhang A, Xiang J. Effects of H_2O on NO emission during oxy-coal combustion with wet recycle. Energy Fuel 2017;31:8392–9. https://doi.org/10.1021/acs.energyfuels.7b00897.
[41] Shah IA, Gou X, Zhang Q, Wu J, Wang E, Liu Y. Experimental study on NO_x emission characteristics of oxy-biomass combustion. J Clean Prod 2018;199:400–10. https://doi.org/10.1016/j.jclepro.2018.07.022.
[42] Ndibe C, Spörl R, Maier J, Scheffknecht G. Experimental study of NO and NO_2 formation in a PF oxy-fuel firing system. Fuel 2013;107:749–56. https://doi.org/10.1016/j.fuel.2013.01.055.
[43] Álvarez L, Riaza J, Gil MV, Pevida C, Pis JJ, Rubiera F. NO emissions in oxy-coal combustion with the addition of steam in an entrained flow reactor. Greenh Gases Sci Technol 2011;1:180–90. 10.1002/ghg.16.
[44] Karlström O, Wu H, Glarborgb P. Influence of H2O on NO formation during char oxidation of biomass. Fuel 2019;235:1260–5. https://doi.org/10.1016/j.fuel.2018.08.156.
[45] Lu P, Hao J, Yu W, Zhu X, Dai X. Effects of water vapor and Na/K additives on NO reduction through advanced biomass reburning. Fuel 2016;170:60–6. https://doi.org/10.1016/j.fuel.2015.12.037.
[46] Schafer S, Bonn B. Hydrolysis of HCN as an important step in nitrogen oxide formation in fluidised combustion, Part 1: homogeneous reactions. Fuel 2000;79:1239–46. https://doi.org/10.1016/S0016-2361(99)00254-9.
[47] Glarborg P, Miller JA, Ruscic B, Klippenstein SJ. Modeling nitrogen chemistry in combustion. Prog Energy Combust Sci 2018;67:31–68. https://doi.org/10.1016/j.pecs.2018.01.002.
[48] Aarna I, Suuberg EM. A review of the kinetics of the nitric oxide-carbon reaction. Fuel 1997;76:475–91. https://doi.org/10.1016/S0016-2361(96)00212-8.
[49] Arenillas A, Rubiera F, Pis JJ. Nitric oxide reduction in coal combustion: role of char surface complexes in heterogeneous reactions. Environ Sci Technol 2002;36:5498–503. https://doi.org/10.1021/es0208198.